Betatron coupling and related impact of radiation

G. Guignard
CERN, Geneva, Switzerland
(Received 31 October 1994)

Linear coupling of vertical and horizontal oscillations in a circular accelerator or collider is analyzed in the presence of solenoidal and tilted-quadrupole fields. An analytical treatment of the coupled motions based on a Hamiltonian formalism is proposed. Solutions are first given explicitly in the absence of synchrotron radiation and then extended to the case of loss of energy and photon emission by the particles. Applications of the derived formulas to a generic accelerator are presented. Finally, pertinent information related to the large electron-positron collider of CERN is conveyed, in which strategies for dealing with a very large, low harmonic, tilted quadrupole are detailed and a particular scheme for the local compensation of solenoids is discussed.

PACS number(s): 41.75.Ht, 41.85.−p, 29.27.−a

I. INTRODUCTION AND SUMMARY

In circular accelerators and colliders of particles, a correct compensation of the betatron coupling is crucial for the ring operation and for the performance. The presence of too strong coupling may indeed induce optics distortions, transfer of oscillations from one plane to the other, tilt of the normal directions in which the betatron motion is again decoupled, beating of the betatron motion, and shifts of the wave numbers or tunes. All these effects perturb the checking and the control of the designed optics and may even confuse diagnostics such as tune measurements when running conditions are particularly sensitive to coupling effects. Also critical is the implication of linear coupling on the performance of an accelerator and the luminosity of a collider, because of its impact on the transverse emittances. When the collider conveys electrons and positrons, like the Large Electron-Positron (LEP) storage ring at CERN, the equilibrium emittances are critically dependent on the combined influence of betatron coupling and synchrotron radiation in the bending magnets. This phenomenon is all the more important in LEP as a good luminosity requires a flat beam, i.e., a vertical emittance many times smaller than the horizontal one. This article therefore presents the observations made on linear coupling during LEP commissioning and the practical means used to control it. It also describes the analytical tools that have been developed to help in understanding the physics of the mechanisms involved, analyzing the measurements done, and designing correction schemes or strategies. Section II gives the general basic formulas governing coupling in absence of radiation and Sec. III shows how to use them for diagnostic purposes. Section IV describes how coupled betatron oscillations are in turn affected by photon emission and energy loss in lepton rings, while Sec. V emphasizes the application to LEP of the treatment presented and the strategy of compensation applied in such a practical case.

II. HAMILTONIAN TREATMENT OF LINEAR COUPLING

A. Sources of coupling and form of the perturbed Hamiltonian [1,2]

Since the perturbation theory gives the possibility to find the exact equations of perturbed betatron motion, it is convenient to consider linear coupling as a perturbation of the transverse particle oscillations. These oscillations can be coupled by three-dimensional magnetic fields of components B_x, B_z, and B_θ (longitudinal). In this notation, x and z are the transverse coordinates, horizontal and vertical, respectively, and $\theta=s/R$ is the angle at the accelerator center, with s as the distance along the beam axis and R as the average radius of the accelerator. Basically, there are two sources of coupling, i.e., skewed-quadrupole and solenoidal field components, keeping in mind that a finite vertical orbit in sextupoles generates a skewed-quadrupole field. Specific examples of magnetic elements that can generate coupling are (i) tilted-quadrupole lenses for which one has

$$K(\theta)=\frac{R^2}{2\beta\rho}\left[\frac{\partial B_x}{\partial x}-\frac{\partial B_z}{\partial z}\right]; \tag{1}$$

(ii) solenoidal fields for which we define

$$S(\theta)=\frac{R}{2B\rho}B_\theta ; \tag{2}$$

(iii) end effects of large solenoids, described by

$$K(\theta)=(2a_s-1)\dot{S} , \tag{3}$$

where a_s characterizes the geometry of the end plates (for horizontal slots $a_s=1$ and for open ends $a_s=\frac{1}{2}$); and (iv) sextupoles with vertical orbit deviations z_0,

$$K(\theta)=-\frac{R^2}{B\rho}\frac{\partial^2 B_z}{\partial x^2}z_0 , \tag{4}$$

where the second derivative of B_z characterizes the sextu-

pole strength.

A three-dimensional field couples the equations of motion in the following way [3]:

$$\ddot{x}+K_1(\theta)x=\frac{R^2}{B\rho}\frac{\partial B_z}{\partial z}z-\frac{R}{B\rho}B_\theta\dot{z}\ ,$$
$$\ddot{z}+K_2(\theta)z=\frac{-R^2}{B\rho}\frac{\partial B_x}{\partial x}x+\frac{R}{B\rho}B_\theta\dot{x}\ , \tag{5}$$

where the derivatives are taken with reference to θ and the functions $K_1(\theta)$ and $K_2(\theta)$ are the forces exerted on the particles by the magnetic field gradients ($K=R^2G/B\rho$). Equations (5) can be rewritten using the definitions (i) and (ii) as well as the property $\mathrm{div}\mathbf{B}=0$, which links together the transverse and the longitudinal derivatives

$$\ddot{x}+K_1(\theta)x=-(K+\dot{S})z-2S\dot{z}\ ,$$
$$\ddot{z}+K_2(\theta)z=-(K-\dot{S})x+2S\dot{x}\ , \tag{6}$$

all the functions depending on the variable θ, in general.

The form of the Hamiltonian H associated with Eqs. (6) can be shown to be

$$H=\tfrac{1}{2}[K_1x^2+K_2z^2+2Kxz+(p_x-Sz)^2+(p_z+Sx)^2]\ . \tag{7}$$

The proof of this comes from writing the subsequent canonical equations

$$\dot{x}=\frac{\partial H}{\partial p_x}=p_x-Sz\ , \tag{8a}$$
$$\dot{p}_x=-\frac{\partial H}{\partial x}=-K_1x-Kz-(p_z+Sx)S\ , \tag{8b}$$
$$\dot{z}=\frac{\partial H}{\partial p_z}=p_z+Sx\ , \tag{8c}$$
$$\dot{p}_z=-\frac{\partial H}{\partial z}=-K_2z-Kx-(p_x-Sz)S\ . \tag{8d}$$

Equations (8a) and (8c) can be solved for p_y and then differentiated with respect to θ. These two successive results can then be included in Eqs. (8b) and (8d). Rearranging the terms gives finally Eqs. (6), proving the validity of our presupposed form (7).

Knowing $H_0=\frac{1}{2}(K_1x^2+K_2z^2+p_x^2+p_z^2)$ for betatron motion, the perturbed Hamiltonian for linear coupling is obtained by subtracting H_0 from H (7),

$$H_1(y,p_y)=[Kxz+Sxp_z-Szp_x+\tfrac{1}{2}S^2(x^2+z^2)]\ , \tag{9}$$

which is a quadratic form in the y,p_y coordinates (y being used generically to represent either x or z).

Perturbation theory imposes then obtaining an explicit form of $U=H_1$, as a function of the constants a_1 and a_2 of the betatron motion. Note that this form is subordinated to the following properties.

(a) H_1 is a quadratic function (9) of the coordinates and momentum conjugates.

(b) The solutions of the unperturbed betatron motion are linear functions of the four constants a_1, $\bar{a}_1$, a_2, and $\bar{a}_2$ and contain oscillatory terms with frequencies Q_x and Q_z, as recalled hereafter

$$x=a_1ue^{iQ_x\theta}+\bar{a}_1\bar{u}e^{-iQ_x\theta}\ ,$$
$$p_x=a_1(\dot{u}+iQ_xu)e^{iQ_x\theta}+\bar{a}_1(\dot{\bar{u}}-iQ_x\bar{u})e^{-iQ_x\theta}\ ,$$
$$z=a_2ve^{iQ_z\theta}+\bar{a}_2\bar{v}e^{-iQ_z\theta}\ ,$$
$$p_z=a_2(\dot{v}+iQ_zv)e^{iQ_z\theta}+\bar{a}_2(\dot{\bar{v}}-iQ_z\bar{v})e^{-iQ_z\theta}\ ,$$

where u and v are the Floquet functions defined in Eq. (11) and a bar above a symbol means complex conjugate.

(c) For circular accelerators and storage rings, the functions K and S, characterizing the linear-coupling perturbation (9), are obviously periodic in θ with period 2π.

Introducing the general solutions of the unperturbed motion into the expression (9) is a standard calculation that provides [1,2]

$$U=\sum_{j,k,l,m=0}^{2}h^{(2)}_{jklm}a_1^j\bar{a}_1^ka_2^l\bar{a}_2^m \times\exp\{i[(j-k)Q_x+(l-m)Q_z]\theta\} \tag{10}$$

with the rules coming from the above properties that the sum $j+k+l+m$ is equal to 2 and any index takes only one of the values 0, 1, or 2. (Note that $\bar{a}$ is the complex conjugate of a.) The coefficients h [2] obviously depend on the Floquet functions u and v (general name w) and on the coupling forces K (1) and S (2). They are given explicitly hereafter [2]

$$h^{(2)}_{2000}=\tfrac{1}{2}S^2u^2,\quad h^{(2)}_{0200}=\tfrac{1}{2}S^2\bar{u}^2,\quad h^{(2)}_{1100}=S^2u\bar{u}\ ,$$
$$h^{(2)}_{0020}=\tfrac{1}{2}S^2v^2,\quad h^{(2)}_{0002}=\tfrac{1}{2}S^2\bar{v}^2,\quad h^{(2)}_{0011}=S^2v\bar{v}\ ,$$
$$h^{(2)}_{1010}=Kuv+S[u(\dot{v}+iQ_zv)-v(\dot{u}+iQ_xu)]\ ,$$
$$h^{(2)}_{1001}=Ku\bar{v}+S[u(\dot{\bar{v}}-iQ_z\bar{v})-\bar{v}(\dot{u}+iQ_xu)]\ , \tag{11}$$
$$h^{(2)}_{0101}=\text{c.c. of } h^{(2)}_{1010},\quad h^{(2)}_{0110}=\text{c.c. of } h^{(2)}_{1001}\ ,$$
$$w=\left[\frac{\beta_y(\theta)}{2R}\right]^{1/2}\exp[i(\mu_y-Q_y\theta)]\ ,$$

where c.c. stands for complex conjugate and w is equal to u for the coordinate x and to v for z. The quantities β_y and μ_y are, respectively, the betatron amplitude and the phase advance in either transverse coordinate x or z.

The property (c) mentioned above makes it possible and judicious to develop the coefficients h [2] in Fourier's series,

$$h^{(2)}_{jklm}(\theta)=\sum_{q=-\infty}^{+\infty}h^{(2)}_{jklmq}e^{iq\theta}\ , \tag{12}$$

with

$$h^{(2)}_{jklmq}=\frac{1}{2\pi}\int_0^{2\pi}h^{(2)}_{jklm}(\theta)e^{-iq\theta}d\theta\ .$$

Putting Eq. (12) into (10) adds another sum over the harmonics q and modifies slightly the phase term or argument $A_{\exp}$ of the exponential function

$$A_{\exp}=i[(j-k)Q_x+(l-m)Q_y+q]\theta\ . \tag{13}$$

Let us introduce now our *first approximation:* we assume, with other authors [4,5], that the low-frequency part of the Hamiltonian (10) gives the important variations of the constants a_1, $\bar{a}_1$, a_2, and $\bar{a}_2$. The low-frequency part corresponds to the special choices of the indices that are canceling the argument (13). The corresponding conditions are

$$j=k, \quad l=m, \quad q=0 ,$$

with j and l taking either the value 0 or 1, and

$$(j-k)Q_x+(l-m)Q_z+q=0$$

as a whole. Redefining $n_1=j-k$, $n_2=l-m$, and $p=-q$, this is equivalent to the well-known resonance condition

$$n_1Q_x+n_2Q_z-p=0 ,$$

where n_1 can take the values 0, 1, or 2 and n_2 the values 0, ±1, or 2 according to selection rules.

With this approximation to the low-frequency part, the Hamiltonian U can be explicitly written [2]

$$\begin{aligned} U=&h^{(2)}_{11000}a_1\bar{a}_1+h^{(2)}_{00110}a_2\bar{a}_2 \ \text{(frequency shift)}+h^{(2)}_{1010-p}a_1a_2e^{i(Q_x+Q_z-p)\theta}+\text{c.c.} \ \text{(sum resonance)} \\ &+h^{(2)}_{1001-p}a_1\bar{a}_2e^{i(Q_x-Q_z-p)\theta}+\text{c.c.} \ \text{(difference resonance)}+h^{(2)}_{2000-p}a_1^2e^{i(2Q_x-p)\theta}+\text{c.c.} \ \text{(horizontal resonance)} \\ &+h^{(2)}_{0020-p}a_2^2e^{i(2Q_z-p)\theta}+\text{c.c.} \ \text{(vertical resonance)} , \end{aligned} \tag{14}$$

where c.c. again stands for complex conjugate. Equations (14) indicate that coupling perturbation implies frequency (or tune) shifts with amplitude, sum and difference coupling resonances, but also one-dimensional quadrupole resonances. However, only sum and difference resonance driving terms are to first order in the perturbation functions (1)–(4), the others being to second order. This can be seen in the expressions of these driving terms, deduced from Eqs. (11)–(13),

$$h^{(2)}_{\substack{11000\\00110}}=\frac{1}{8\pi R}\int_0^{2\pi}S^2\beta_y d\theta , \tag{15a}$$

$$h^{(2)}_{\substack{2000\\0020}-p}=\frac{1}{8\pi R}\int_0^{2\pi}S^2\beta_y e^{i[2\mu_y-(2Q_y-p)\theta]}d\theta , \tag{15b}$$

$$\begin{aligned} h^{(2)}_{\substack{1001\\1010}-p}=&\frac{1}{4\pi R}\int_0^{2\pi}\sqrt{\beta_x\beta_z}\left[K+RS\left[\frac{\alpha_x}{\beta_x}-\frac{\alpha_z}{\beta_z}\right]-iRS\left[\frac{1}{\beta_x}\pm\frac{1}{\beta_z}\right]\right] \\ &\times\exp\{i[(\mu_x\mp\mu_z)-(Q_x\mp Q_z-p)\theta]\}d\theta , \end{aligned} \tag{15c}$$

where the coordinate y (x or z) and the sign in the expression (15) have to be chosen according to the indices of $h^{(2)}$ (x and top sign with the upper indices and vice versa).

For the first-order (in the perturbation function) resonances, coupling coefficients proportional to the driving terms can be written by definition [2,6],

$$C^+=2h^{(2)}_{1010-p}, \quad C^-=2h^{(2)}_{1001-p} \tag{16}$$

with, in addition,

$$\Delta^{\mp}=Q_x\mp Q_z-p, \quad \lambda_x=h^{(2)}_{11000}, \quad \lambda_z=h^{(2)}_{00110} . \tag{17}$$

Effects of coupling are then frequency shifts and excitation of several resonances. Equations of motion of the type (8) can be written using $\bar{a}_1,\bar{a}_2$ for the positions and ia_1,ia_2 for momenta. Explicit solutions have been calculated [2] for each resonance separately, including the second-order (in the perturbation function) tune shifts (characterized by λ_x and λ_z).

B. Solution of coupled motion near a single resonance [2]

It is possible to find the explicit solutions for every resonance excited by linear-coupling sources, i.e., Q_x-Q_z, Q_x+Q_z, $2Q_x$, and $2Q_z$, which are all of second order in the wave numbers (this order being defined by the absolute-value sum of n_1 and n_2, the coefficients of the tunes). Taking separately each resonance and including the terms λ_x and λ_z of Eqs. (17), let us first deal with the two more important sum and difference resonances, which are to first order in the perturbation $K(\theta)$ and $S(\theta)$.

Introducing the expression (14) of U for one single resonance at the time in the equations of motion and using the definitions (16) and (17), the explicit equations of motion can be written in either case of a dominant sum resonance or difference resonance

$$\frac{da_1}{d\theta}=i\lambda_x a_1+if_a e^{-i\theta\Delta} , \tag{18a}$$

$$\frac{da_2}{d\theta}=i\lambda_z a_2+ig_a e^{\pm i\theta\Delta} , \tag{18b}$$

where one has introduced

(i) $f_a=\frac{1}{2}\bar{C}^- a_2,\quad g_a=\frac{1}{2}C^- a_1$

for the difference resonance and

(ii) $f_a=\frac{1}{2}\bar{C}^+ \bar{a}_2,\quad g_a=\frac{1}{2}\bar{C}^+ \bar{a}_1$

for the sum resonance. The sign + or − of the exponent in Eq. (18b) concerns case (i) or (ii) and Δ is equal to Δ^- or Δ^+, respectively.

Equations (18) are the manifestation of our *second approximation:* we assume that the working point $\{Q_x,Q_z\}$ is close enough to one resonance due to coupling and remote from the others, so that one can keep only the corresponding term of U. To be able to solve explicitly the equations of motion, this approximation is required, but to compensate coupling effects both resonance driving terms (16) can simultaneously be canceled.

Since λ_x and λ_z are real quantities, we can make the following change in the variables in order to solve (18):

$$a_1=b_1e^{i\lambda_x\theta},\quad a_2=b_2e^{i\lambda_z\theta}. \tag{19}$$

Putting (19), which is the solution of (18) for $C^-=0$ or $C^+=0$, in (18) gives the equations for b_1 and b_2

$$\frac{db_1}{d\theta}=if_be^{-iD\theta},\quad \frac{db_2}{d\theta}=ig_be^{\pm iD\theta}, \tag{20}$$

where f_b and g_b are defined as f_a and g_a in items (i) and (ii) above, after replacing a_1,a_2 by b_1,b_2 and the appropriate sign is chosen according to the resonance considered. The coefficient D has also a definition that depends on the resonance and the whole thing can be summarized as follows: for (i) the difference resonance

$$f_b=\tfrac{1}{2}\bar{C}^- b_2,\quad g_b=\tfrac{1}{2}C^- b_1,\quad D=\Delta^-+\lambda_x-\lambda_z$$

and for (ii) the sum resonance

$$f_b=\tfrac{1}{2}\bar{C}^+ \bar{b}_2,\quad g_b=\tfrac{1}{2}\bar{C}^+ \bar{b}_1,\quad D=\Delta^++\lambda_x+\lambda_z\ .$$

The set of equations (20) can be relieved of the exponential functions by introducing a new variable marked $b_2^\sim$ and defined by

$$b_2^\sim=b_2e^{\mp iD\theta}, \tag{21}$$

as shown in the results

$$\frac{db_1}{d\theta}=if_{b^\sim}$$

with $f_{b^\sim}=\frac{1}{2}\bar{C}^- b_2^\sim$ or $\frac{1}{2}\bar{C}^+\bar{b}_2^\sim$,

$$\frac{db_2^\sim}{d\theta}=\tfrac{1}{2}iC^- b_1-iDb_2^\sim \tag{22}$$

for the difference resonance, and

$$\frac{d\bar{b}_2^\sim}{d\theta}=-\tfrac{1}{2}iC^+ b_1-iD\bar{b}_2^\sim$$

for the sum resonance. Combining the equation for b_1 with either the first (difference resonance) or the second (sum resonance) equation for $b_2^\sim$, it is possible to write a second-order equation for either the difference or the sum resonance, respectively,

$$\begin{aligned}&\frac{d^2b_2^\sim}{d\theta^2}+iD\frac{db_2^\sim}{d\theta}+\frac{C^-\bar{C}^-}{4}b_2^\sim=0\ ,\\ &\frac{d^2\bar{b}_2^\sim}{d\theta^2}+iD\frac{d\bar{b}_2^\sim}{d\theta}-\frac{C^+\bar{C}^+}{4}\bar{b}_2^\sim=0\ .\end{aligned} \tag{23}$$

The solutions of these two equations solve the perturbation problem defined in Sec. II A and are very similar, since the equations are themselves similar. One obtains

$$\begin{aligned}&b_1=\frac{1}{2}\bar{C}\left[\frac{B_1}{\omega_2}e^{i\omega_2\theta}+\frac{B_2}{\omega_1}e^{i\omega_1\theta}\right]\\ &b_2^\sim\ \text{or}\ \bar{b}_2^\sim=B_1e^{-i\omega_1\theta}+B_2e^{-i\omega_2\theta}\end{aligned} \tag{24}$$

with the definition of the ω's, for the difference and the sum resonance, respectively,

$$\begin{aligned}&\omega_{1,2}=\tfrac{1}{2}[-D\pm\sqrt{D^2+|C^-|^2}]\ ,\\ &\omega_{1,2}=\tfrac{1}{2}[-D\pm\sqrt{D^2-|C^+|^2}]\ ,\end{aligned} \tag{25}$$

where the indices 1,2 are associated with the double sign in front of the square root and D is defined in the paragraph below Eq. (20). At times, for convenience, one introduces by definition $\eta^\mp=\sqrt{D^2\pm|C^\mp|^2}$. The quantities B_1 and B_2 are now the actual complex constants of the perturbed motion.

Moving backwards through Eqs. (24), (21), and (19), one can write the variation with θ of the constants a_1 and a_2 of the unperturbed motion, in the case of linear betatron coupling. Near a single *difference resonance* one has

$$\begin{aligned}&a_1=\frac{1}{2}\bar{C}^-\left[\frac{B_1}{\omega_2}e^{i\omega_{x2}\theta}+\frac{B_2}{\omega_1}e^{i\omega_{x1}\theta}\right],\\ &a_2=B_1e^{-i\omega_{z2}\theta}+B_2e^{-i\omega_{z1}\theta},\end{aligned} \tag{26}$$

where the wave numbers ω depend now not only on the sign in (25) but also on the plane considered, by virtue of (19) that implies $\lambda_x\neq\lambda_z$, $\lambda_x\neq0$, and $\lambda_z\neq0$,

$$\begin{aligned}\omega_{x1,2}&=\tfrac{1}{2}[-(\Delta^--\lambda_x-\lambda_z)\\ &\qquad\pm\sqrt{(\Delta^-+\lambda_x-\lambda_z)^2+|C^-|^2}]\ ,\\ \omega_{z1,2}&=\tfrac{1}{2}[-(\Delta^-+\lambda_x+\lambda_z)\\ &\qquad\mp\sqrt{(\Delta^-+\lambda_x-\lambda_z)^2+|C^-|^2}]\ .\end{aligned} \tag{27}$$

These equations indicate that in this case the motion is always stable with amplitude beating and exchange between the two transverse directions. Similarly, near a single *sum resonance* one can write

$$\begin{aligned}&a_1=\frac{1}{2}\bar{C}^+\left[\frac{B_1}{\omega_2}e^{i\omega_{x2}\theta}+\frac{B_2}{\omega_1}e^{i\omega_{x1}\theta}\right],\\ &a_2=\bar{B}_1e^{i\omega_{z1}\theta}+\bar{B}_2e^{i\omega_{z2}\theta}\end{aligned} \tag{28}$$

and the wave numbers are slightly different from (27),

$$\omega_{x1,2}=\tfrac{1}{2}[-(\Delta^+-\lambda_x+\lambda_z) \pm\sqrt{(\Delta^++\lambda_x+\lambda_z)^2-|C^+|^2}]\,,$$
$$\omega_{z1,2}=\tfrac{1}{2}[-(\Delta^++\lambda_x+\lambda_z) \pm\sqrt{(\Delta^++\lambda_x+\lambda_z)^2-|C^+|^2}]\,. \quad (29)$$

These last expressions indicate that the motion near a sum resonance can be stable or unstable, depending on the amplitude of $|C^+|$. It is stable if ω_x and ω_z are real. In other words, this means that if $|C^+|\le|\Delta^++\lambda_x+\lambda_z|$, the motion is stable, and if $|C^+|>|\Delta^++\lambda_x+\lambda_z|$, the motion is unstable. When the motion is unstable, amplitudes may increase to infinity in both transverse directions.

The forms of Eqs. (26)–(29) show that the perturbed betatron motion is made of two modes associated with two different frequencies ω_1 and ω_2. Results (27) and (29) show moreover that the inclusion of the S^2 terms from the Hamiltonian, i.e., λ_x and λ_z, only slightly modifies the frequencies of the two modes and that this effect is different from the horizontal and the vertical mode. In the special case where the terms λ_x and λ_z are neglected, Eqs. (27) and (29) simplify to

$$\omega_{1,2}=\tfrac{1}{2}[-\Delta^-\pm\sqrt{\Delta^{-2}+|C^-|^2}]=\tfrac{1}{2}[-\Delta^-\pm\eta^-]\,, \quad (30a)$$
$$\omega_{1,2}=\tfrac{1}{2}[-\Delta^+\pm\sqrt{\Delta^{+2}-|C^+|^2}]=\tfrac{1}{2}[-\Delta^+\pm\eta^+] \quad (30b)$$

and become independent of the plane considered.

Considering now only a difference resonance and neglecting the tune shifts with amplitude λ_x and λ_z according to Eq. (30a), the complete solution can be deduced from the general form of the solutions of the unperturbed motion (see Ref. [2]). Dealing only with the amplitudes and ignoring for simplicity the conjugate momenta, the solution is

$$x(\theta)=\frac{1}{2}\bar{C}-\left[\frac{B_1}{\omega_2}e^{i\omega_2\theta}+\frac{B_2}{\omega_1}e^{i\omega_1\theta}\right]\left[\frac{\beta_x}{2R}\right]^{1/2}e^{i\mu_x}+\text{c.c.}\,,$$
$$z(\theta)=(B_1e^{-i\omega_1\theta}+B_2e^{-i\omega_2\theta})\left[\frac{\beta_z}{2R}\right]^{1/2}e^{i\mu_z}+\text{c.c.} \quad (31)$$

With these equations, we went as far as possible in dealing with linear coupling by using perturbation theory with the Hamiltonian formalism.

Before closing this section, let us make two more remarks. The first one concerns the effects related to λ_x and λ_z. Considering as an example the situation where C^- is vanishing after compensation, the solution of the motion must now include the constants (19) and therefore Eq. (31) is replaced by

$$x(\theta)=b_1\left[\frac{\beta_x}{2R}\right]^{1/2}e^{i(\mu_x+\lambda_x\theta)}+\text{c.c.}\,,$$
$$z(\theta)=b_2\left[\frac{\beta_z}{2R}\right]^{1/2}e^{i(\mu_z+\lambda_z\theta)}+\text{c.c.} \quad (32)$$

The effects referred to are different tune shifts in the two transverse directions, the amplitudes of which are given by Eq. (15a), hence proportional to the square of $S(\theta)$ and to betatron amplitude. Therefore, one has to keep in mind that it might be necessary to adjust the tunes after compensation of solenoidal fields with tilted quadrupoles.

The second remark concerns the one-dimensional resonances $2Q_y-p$, which are considered to be less important because they are to second order in the perturbation $S(\theta)$. In fact, large stop bands are opened near each integer or half integer by the strong quadrupoles of the nominal lattice, responsible for $K_{1,2}$. The effect of $S(\theta)$ in this respect is just to slightly modify the forbidden bandwidths around these particular values, i.e., the quadrupole driving terms, according to

$$\kappa=\frac{1}{8\pi R}\int_0^{2\pi}(K_{1,2}+S^2)\beta_y e^{i[2\mu_y-(2Q_y-p)\theta]}d\theta\,. \quad (33)$$

Usually S^2 is small with respect to the nominal $K_{1,2}$ and therefore negligible. But a judicious compensation of the tune shifts (32) mentioned might also be able to cancel the effects on κ if the corresponding change $\Delta K_{1,2}$ balances the S^2 term in (33).

III. MEASURING THE DIFFERENCE COUPLING COEFFICIENT

The solutions of the linearly coupled motions (31) give a clue to possible methods for measuring the coupling coefficient C^- of the difference resonance. Using the form of the coupled motions following a dipole kick in one transverse direction, one can show that the subsequent coherent oscillations can be analyzed for measuring the real and the imaginary part of this complex coefficient. More generally, considering the two frequency modes (30) that characterize the motions (31) and mapping out their separation as a function of the tunes can be used for measuring the module $|C^-|$. These two methods are described below.

A. Coupling measurement from coherent oscillations [7–9]

Let us summarize the analysis of the transverse oscillations after kicking the beam horizontally, the details of which can be found in Ref. [7]. The equations of motion (31) are functions of two complex constants (four real constants) that can be defined from the initial conditions of the motion. According to our assumption, these conditions are

$$x_0=z_0=\dot{z}_0=0,\quad \dot{x}_0\neq0\,. \quad (34)$$

Now it is useful to rewrite (31) by using the sinusoidal functions and bringing into evidence the two modes characterized by the frequencies ω_1 and ω_2,

$$
\begin{aligned}
x=&\left[\frac{4R^2}{\beta_{x_0}\beta_{z_0}}-C_1^2\right]^{-1}\frac{\sqrt{\beta_x}}{\eta}\\
&\times[d_1\cos(\mu_x+\omega_1\theta)-e_1\sin(\mu_x+\omega_1\theta)\\
&\quad -d_2\cos(\mu_x+\omega_2\theta)+e_2\sin(\mu_x+\omega_2\theta)]\ ,\\
z=&\left[\frac{4R^2}{\beta_{x_0}\beta_{z_0}}-C_1^2\right]^{-1}\frac{\sqrt{\beta_z}}{\eta}\\
&\times[f_1\cos(\mu_z-\omega_2\theta)-g_1\sin(\mu_z-\omega_2\theta)\\
&\quad -f_2\cos(\mu_z-\omega_1\theta)+g_2\sin(\mu_z-\omega_1\theta)]\ ,
\end{aligned}
\tag{35}
$$

where β_{x0},β_{z0} are the betatron amplitudes at the kicker position, C_1,C_2 the real and imaginary parts of C^-, d, e, f, and g new constants of motion, and η is equal to η^-, defined after Eq. (25) or in (30). After some cumbersome algebra [7], it is possible to write the constants as functions of the initial conditions (34),

$$
\begin{aligned}
d_{1,2}&=\frac{C_1C_2}{\sqrt{\beta_{x_0}}}\dot{x}_0\ ,\\
e_{1,2}&=-\left[\frac{R|C^-|^2}{\omega_{1,2}\beta_{z_0}}-C_1^2\right]\frac{\dot{x}_0}{\sqrt{\beta_{x_0}}}\ ,\\
f_{1,2}&=2\frac{RC_2}{\beta_{z_0}\sqrt{\beta_{x_0}}}\dot{x}_0\ ,\\
g_{1,2}&=-2C_1\left[\frac{R}{\beta_{z,0}}-\omega_{1,2}\right]\frac{\dot{x}_0}{\sqrt{\beta_{x_0}}}\ .
\end{aligned}
\tag{36}
$$

One observes from (35) that the single-particle motion contains fast and slow oscillations associated with the phase μ_y and $\omega_{1,2}\theta$, respectively. It is therefore possible, using the combination law of sinusoidal functions, to factorize the signal into a slowly oscillating envelope and a fast oscillating component [7]. The result is

$$
\begin{aligned}
x(\theta)&=\frac{\sqrt{\beta_x}}{\eta}E_x\cos\left[\mu_x-\frac{\Delta}{2}\theta-\phi_x\right]\ ,\\
z(\theta)&=\frac{\sqrt{\beta_z}}{\eta}E_z\cos\left[\mu_z+\frac{\Delta}{2}\theta-\phi_z\right]\ ,
\end{aligned}
\tag{37}
$$

where both the phases ϕ_x,ϕ_z and the envelopes E_x,E_z are functions of the coefficients d, e, f, and g and Δ stands for the distance (17) from the difference resonance "measured." In the particular case of a horizontal kick, with the particular coefficients (36), the envelopes become, after neglecting the terms containing $|C|\beta_{z0}/R$ ($\ll 1$),

$$
\begin{aligned}
E_x^2&=\frac{\beta_{x_0}}{R^2}\left[\eta^2-|C^-|^2\sin^2\frac{\eta}{2}\theta\right]\dot{x}_0^2\ ,\\
E_z^2&=\frac{\beta_{x_0}}{R^2}|C^-|^2\sin^2\frac{\eta}{2}\theta\,\dot{x}_0^2\ .
\end{aligned}
\tag{38}
$$

It comes out from Eq. (38) that the fraction F of the energy (taken here as the square of the envelope amplitudes) interchanged between the two signals, the ratio G of the minimum to the maximum of the horizontal envelope and the period T of the envelope oscillations (involving the revolution frequency f_{rev}) are

$$
\begin{aligned}
F&=\frac{|C^-|^2}{\eta^2}=\frac{|C^-|^2}{\Delta^2+|C^-|^2}\ ,\\
G&=\frac{|\Delta|}{\eta}=\frac{|\Delta|}{\sqrt{\Delta^2+|C^-|^2}}\ ,\\
T&=\frac{1}{\eta f_{\text{rev}}}\ ,
\end{aligned}
\tag{39}
$$

in agreement with Refs. [7] and [8]. It is interesting to note that the maxima and minima of the envelopes (38) appear for $\eta\theta=n\pi$, n being an integer, and that these envelopes are independent of the phase of C^- in the complex plane, if the assumption $R/\beta_{z0}\gg|C^-|$ is verified. Consequently, the knowledge of C_1 and C_2 requires complementary measurements, such as the response to an inclined kick, for instance,

$$
x_0=z_0=0\ ,\qquad \dot{x}_0\neq 0,\quad \dot{z}_0\neq 0,\quad \dot{x}_0/\dot{z}_0=\sqrt{\beta_{z_0}/\beta_{x_0}}\ .
\tag{40}
$$

More precisely, the coherent oscillations following a horizontal kick have the characteristics shown in Fig. 1 [9], according to Eqs. (38). In the plane parallel to the kick, the initial amplitude of the envelope is finite ($\dot{x}_0\neq 0$) while it is zero in the orthogonal plane. With the time, the envelopes beat with the period T and the horizontal one has minima when the vertical one has maxima. This illustrates the interchange of energy already mentioned, in the presence of second-order (in tune) difference resonance. Easily measured are the period T and the ratio G of the minimum to the maximum of the horizontal amplitude. Solving Eqs. (39), such measurements give the distance from, and the driving term of, the resonance

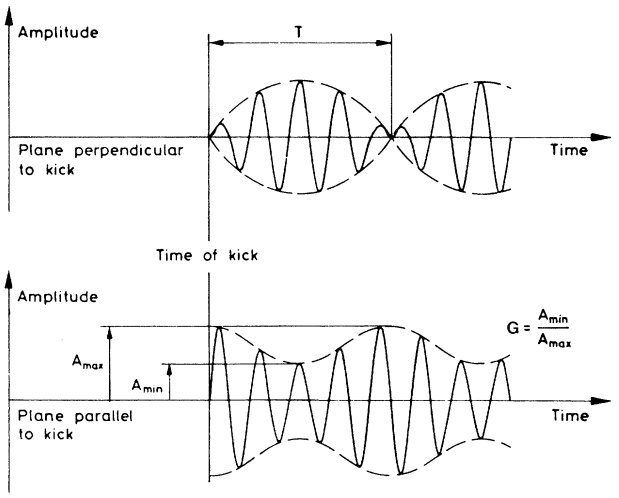

FIG. 1. Coherent oscillations following a horizontal kick (arbitrary units).

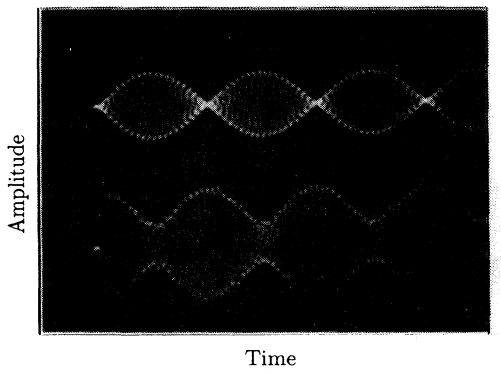

FIG. 2. Vertical (above) and horizontal (below) coherent oscillations measured in the Intersecting Storage Rings (CERN) after a horizontal kick. The beating period is 0.5 ms in this case.

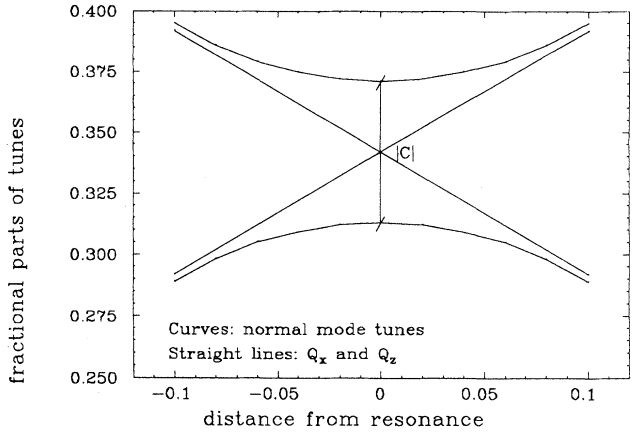

FIG. 3. Coupled tunes as functions of the distance from the difference resonance (dimensionless quantities).

$$|\Delta|=\frac{G}{Tf_{\text{rev}}},\quad |C^-|=\frac{1}{Tf_{\text{rev}}}\sqrt{1-G^2}\,, \tag{41}$$

[where f_{rev} is the revolution frequency].

As an illustration of a practical use of this method, Fig. 2 shows one of the first signals obtained in the now dismantled Intersecting Storage Rings (ISR, at CERN) from the filter output of the device that was used to measure the tunes (kicker and large band pickup). It is clear from this picture that the coherency of these signals (proton beam) was more than sufficient to measure T and G with very good accuracy. This question of coherency has to be considered when designing a coupling meter, in particular for an electron beam, and the kicker has to be strong enough to generate oscillations of amplitude that are large with respect to the pickup resolution. The revolution frequency does not limit the precision of this method since it is usually known to a high accuracy. In the case of Fig. 2, the measured value was $|C^-|=1.2\times10^{-2}$ and corresponded to the residual coupling of the ring plus the contribution of one experimental solenoid.

In the ISR, the carrier frequency was 30–300 kHz and modulation frequency 0.5–10 kHz. The pickup signal was passing through a rectifier, followed by a sharp-edge, low-pass filter, and differentiated. The zero crossings were used for measuring T and triggering units that stored maxima and minima of the signal. The precision was $\pm3\%$ for the maximum and the minimum values and $\pm1\%$ for T, giving about 4% on $|C^-|$ and $|\Delta|$.

B. Coupling measurements from mode frequencies

Solving the equations of motion for a difference resonance revealed the existence of two modes at frequencies ω_1 and ω_2 (35). The positions x and z are given by a mixture of these modes, but it is possible to rotate the initial axes until the modes are decoupled. These inclined modes are termed normal modes. According to Eq. (30a), which gives the frequencies of these modes when λ_x and λ_z are neglected, their wave numbers are separated by $\eta/2$, i.e.,

$$\begin{aligned} Q_{n,m,1}&=Q_x-\frac{\Delta}{2}+\frac{1}{2}\sqrt{\Delta^2+|C^-|^2}\,,\\ Q_{n,m,2}&=Q_z+\frac{\Delta}{2}-\frac{1}{2}\sqrt{\Delta^2+|C^-|^2}\,, \end{aligned} \tag{42}$$

where only the fractional parts of the tunes are included. When $|C^-|=0$, the normal mode tunes are equal to the unperturbed betatron tunes Q_x and Q_z. When $|C^-|\neq0$, the effects on the normal mode tunes depend on Δ $(=Q_x-Q_z)$. If Δ is large with respect to $|C^-|$, there is little change of the tunes, but when Δ is small the impact of coupling increases, to reach a maximum at $\Delta=0$ (with the tune split equal to $|C^-|$). This frequency split of the normal modes is associated with the above mentioned rotation of the normal axes and sometime an elliptical polarization if $C_2\neq0$.

These effects can be observed experimentally. Increasing Q_x and reducing Q_z in the vicinity of the coupling resonance while also measuring the tunes with horizontal and vertical kickers and pickups will result in curves similar to those of Fig. 3. The pickups react indeed at the frequencies of the normal modes 1 and 2 and one can distinguish three typical situations: (a) $|C^-|<\Delta$, where the modes are nearly vertical and horizontal and the pickup measurements are reliable; (b) $|C^-|\approx\Delta$, where difficulties in measuring the tunes begin to appear and tune readings start to jump back and forth from mode 1 to mode 2 [two lines are visible on each (horizontal or vertical) pickup]; and (c) $|C^-|>\Delta$, where tune readings are spanning the stop band visible in Fig. 3 (at $\Delta\approx0$, the pickups respond equally well to both modes, which are now at 45°). This shows that the difference in normal mode frequencies is exactly equal to $|C^-|$ when $\Delta=0$ and that measuring the tunes while scanning the resonance vicinity provides another way of measuring $|C^-|$.

IV. AMPLITUDE VARIATION DUE TO RADIATION AND ACCELERATION

A. General expression of the amplitude variation

Considering the expression (31) for a difference resonance and including now the conjugate momenta $p_x=\dot{x}+Sz$ and $p_z=\dot{z}-Sx$, the entire solution for the vector $\mathbf{Y}=(x,p_x,z,p_z)$ can be written as follows in presence of linear coupling:

$$Y_j=\sum_{k=1}^{4} w_{jk}(\theta)A_k, \quad j=1,\ldots,4 , \tag{43}$$

where j is numbering the four components of $\mathbf{Y}$,

$$A_1=B_1, \quad A_2=\bar{B}_1, \quad A_3=B_2, \quad A_4=\bar{B}_2 ,$$

and the functions w are

$$\begin{aligned}
w_{\substack{11\\13}}&=\frac{\bar{C}-}{2\omega_{\substack{2\\1}}}\left[\frac{\beta_x}{2R}\right]^{1/2} e^{i(\mu_x+\omega_{\substack{2\\1}}\theta)} ,\\
w_{\substack{21\\23}}&=\frac{\bar{C}-}{2\omega_{\substack{2\\1}}}\left[\frac{R}{2\beta_x}\right]^{1/2}(i-\alpha_x)e^{i(\mu_x+\omega_{\substack{2\\1}}\theta)} ,\\
w_{\substack{31\\33}}&=\left[\frac{\beta_z}{2R}\right]^{1/2} e^{i(\mu_z-\omega_{\substack{1\\2}}\theta)} ,\\
w_{\substack{41\\43}}&=\left[\frac{R}{2\beta_z}\right]^{1/2}(i-\alpha_z)e^{i(\mu_z-\omega_{\substack{1\\2}}\theta)} ,\\
w_{j2}&=\bar{w}_{j1}, \quad w_{j4}=\bar{w}_{j3} .
\end{aligned} \tag{44}$$

The two different subscripts of the w's are associated with the two indices of ω and the form of the functions (44) implies that the following relations hold:

$$w_{jk}(\theta+2\pi)=w_{jk}(\theta)e^{i2\pi\lambda_{jk}} \tag{45}$$

with

$$\lambda_{j2}=-\lambda_{j1}, \quad \lambda_{j4}=-\lambda_{j3} .$$

These solutions are strictly valid in the absence of radiation, but coupled betatron oscillations of leptons are in turn enhanced by photon emission and damped by the longitudinal acceleration as well as by the average energy loss in the presence of the focusing component of the magnetic field.

Starting from the constants A_k of the coupled motion, we now look for their variations due to these effects [10]. *Assuming* that these constants change slowly with respect to the quantum fluctuations and the period of the coupled betatron oscillations, they will reach an equilibrium between excitation and damping after a few damping times. It is precisely these equilibrium values of A_k that we want to derive in the following subsections.

It follows from Eq. (44) that the quantity F defined below is an invariant of the motion

$$F(w_{jl},w_{jk})=w_{1l}w_{2k}-w_{2l}w_{1k}+w_{3l}w_{4k}-w_{4l}w_{3k} . \tag{46}$$

As a consequence of the invariance of F and of the properties (45), we can write

$$\begin{aligned}
F[w_{jl}(\theta),w_{jk}(\theta)]&=F[w_{jl}(\theta+2\pi),w_{jk}(\theta+2\pi)]\\
&=\exp[i2\pi(\lambda_{jl}+\lambda_{jk})]\\
&\quad\times F[w_{jl}(\theta),w_{jk}(\theta)]
\end{aligned} \tag{47}$$

and the equality between the first and the last term of Eq. (47) (which can only be satisfied if the exponential is equal to 1) induces the orthonormality

$$\begin{aligned}
F(w_{jl},w_{jk})&=1 \quad \text{if } w_{jl}=\bar{w}_{jk} ,\\
F(w_{jl},w_{jk})&=0 \quad \text{if } w_{jl}\neq\bar{w}_{jk} .
\end{aligned} \tag{48}$$

This property of orthonormality can now be used to solve Eq. (43) for the A_k's. Let us write indeed

$$F(Y_j,w_{jk})=\sum_{l=1}^{4} A_l F(w_{jl},w_{jk})=\bar{A}_k F(\bar{w}_{jk},w_{jk}) , \tag{49}$$

making use of Eqs. (43) and (48). Then we derive from the equality (49)

$$A_k=\frac{F(Y_j,\bar{w}_{jk})}{F(w_{jk},\bar{w}_{jk})} . \tag{50}$$

Since we want to look for the variations of the A_k's due to changes in the canonical variables (vector Y), Eq. (50) is the key equation. In general, any variation of $|A_k|$ due to trajectory changes δY_j can be expressed as

$$\begin{aligned}
\delta|A_k|^2&=\bar{A}_k\delta A_k+A_k\delta\bar{A}_k+|\delta A_k|^2\\
&=\frac{1}{F(w_{jk},\bar{w}_{jk})}\left\{\bar{A}_k F(\delta Y_j,\bar{w}_{jk})-A_k F(\delta Y_j,w_{jk})\right.\\
&\quad-\frac{1}{F(w_{jk},\bar{w}_{jk})}F(\delta Y_j,\bar{w}_{jk})\\
&\quad\left.\times F(\delta Y_j,w_{jk})\right\} .
\end{aligned} \tag{51}$$

B. Application to photon emission and acceleration

Considering the photon emission, it is well known [11] that the equilibrium orbit and the betatron variables are changed by a quantity that is proportional to the photon energy ε and to the dispersion $\mathbf{D}$, whose components are $(D_x,\dot{D}_x,D_z,\dot{D}_z)$:

$$\partial\mathbf{Y}=\frac{\varepsilon}{E_0}\mathbf{D} . \tag{52}$$

In the presence of longitudinal acceleration δE in a cavity, only the transverse momenta are changed while the transverse coordinates remain constant:

$$\delta\mathbf{Y}=(\delta x,\delta p_x,\delta z,\delta p_z)=(0,-p_x,0,-p_z)\frac{\delta E}{E_0} , \tag{53}$$

E_0 being the nominal energy.

Let us first deal with the orbit change due to photon

emission. Since $\delta\mathbf{Y}$ is proportional to ε [Eq. (52)] and since δYj appears linearly as well as quadratically in Eq. (51), it is necessary to evaluate the average $\langle\varepsilon\rangle$ and the mean square $\langle\varepsilon^2\rangle$ of the quantum emission, over a time interval Δt, and to multiply both by the mean emission rate N. We will now consider successively these two terms.

(a) If P_γ stands for the rate of loss of energy by radiation, we have

$$N\Delta t\langle\varepsilon\rangle=\frac{1}{c}P_\gamma\Delta l\ , \tag{54}$$

where Δl is the path length interval and

$$P_\gamma=\frac{2}{3}r_e c\gamma^3 E\frac{1}{\rho^2},\quad \Delta l=\Delta s\left[1+\frac{x}{\rho_x}+\frac{z}{\rho_z}\right]\ . \tag{55}$$

The quantity $1/\rho^2$ in P_γ is proportional to the square of the field B^2. Taking into account the possible presence of field gradients, we must develop B^2 in a series for x and z. Keeping only first-order terms,

$$\frac{B^2}{B_0^2}=1+G_x x+G_z z\ , \tag{56}$$

with

$$G_x=\frac{2}{B_0^2}\left[B_z\frac{\partial B_z}{\partial x}-B_x\frac{\partial B_z}{\partial z}\right],$$

$$G_z=\frac{2}{B_0^2}\left[B_x\frac{\partial B_z}{\partial x}+B_z\frac{\partial B_z}{\partial z}\right].$$

Regrouping all the first-order terms in x and z that appear in the product $P_\gamma\Delta l$, we obtain

$$\frac{1}{c}P_\gamma\Delta l=\frac{1}{c}P_{\gamma 0}\Delta s(1+C_x x+C_z z)\ , \tag{57}$$

with $C_x=1/\rho_x+G_x$ and $C_z=1/\rho_z+G_z$. On the right-hand side, $P_{\gamma 0}$ is calculated on the central trajectory $x=z=0$ with the nominal field B_0.

Putting all these results together and replacing x and z by their development in eigenfunctions [Eq. (43)], the expression we are looking for is

$$N\Delta t\langle\varepsilon\rangle=\Delta t P_{\gamma 0}\left[1+\sum_{k=1}^{4}A_k(C_x w_{1k}+C_z w_{3k})\right]\ . \tag{58}$$

(b) If Q_ε stands for the mean value of the product $N\langle\varepsilon^2\rangle$, we have simply

$$N\Delta t\langle\varepsilon^2\rangle=\Delta t Q_\varepsilon \tag{59}$$

with

$$Q_\varepsilon=\frac{55}{24\sqrt{3}}r_e hc^2\gamma^6 E\frac{1}{\rho^3}\ . \tag{60}$$

In the expression (51) for the amplitude variation, we still need to evaluate the function $F(\delta Y_j,w_{jk})=\varepsilon F(D_j/E_0,w_{jk})$ and the similar one $F(\delta Y_j,\bar{w}_{jk})$. This is simple if we make use of the definition (46):

$$F(D_j/E_0,w_{jk})=\frac{1}{E_0}(D_x w_{2k}-\dot{D}_x w_{1k}+D_z w_{4k}-\dot{D}_z w_{3k})\ . \tag{61}$$

Let us now turn to the question of longitudinal acceleration δE [Eq. (53)]. For the same reasons previously evoked, linear and quadratic terms in δE will be present in Eq. (51). If the quadratic term δE^2 becomes negligible towards the limit $\Delta t\to 0$, the linear term averages to (using eigenfunctions again)

$$\delta p_y=-\frac{\langle\delta E\rangle}{E_0}p_y=-\frac{\langle\delta E\rangle}{E_0}\sum_{k=1}^{4}w_{\substack{2k\\4k}}(\theta)A_k\ . \tag{62}$$

Introducing Eq. (62) in the linear terms of Eq. (51) and assuming logically that the average $\langle\delta E\rangle$ must exactly compensate for the radiation loss gives

$$\delta|A_k|^2_{\text{accel}}=-\frac{P_{\gamma 0}\Delta t}{E_0}|A_k^2|\ . \tag{63}$$

Putting together Eqs. (58), (59), and (61) into Eq. (51) for the photon emission effect and adding the contribution (63) of the acceleration, we can derive the following expression for the amplitude variation:

$$\langle\delta|A_k|^2\rangle=-\frac{P_\gamma\Delta t}{E_0}|A_k^2|-\frac{P_\gamma\Delta t}{E_0}\frac{|A_k^2|}{F(w_{jk},\bar{w}_{jk})}2i\langle\mathrm{Im}[(C_x\bar{w}_{1k}+C_z\bar{w}_{3k})(D_x w_{2k}-\dot{D}_x w_{1k}+D_z w_{4k}-\dot{D}_z w_{3k})]\rangle$$
$$-\frac{Q_\varepsilon\Delta t}{E_0^2F^2(w_{jk},\bar{w}_{jk})}\langle|D_x w_{2k}-\dot{D}_x w_{1k}+D_z w_{4k}-\dot{D}_z w_{3k}|^2\rangle\ . \tag{64}$$

The equality $\bar{A}F(\delta Y,\bar{w})-AF(\delta Y,w)=-2i\,\mathrm{Im}[\bar{A}F(\delta Y,\bar{w})]$ has been applied and the subscript 0 of P_γ abandoned for simplicity. The three terms of (64) give, respectively, the amplitude variation associated with acceleration, radiation damping, and quantum excitation.

C. Equilibrium amplitudes with coupling and radiation

The finite amplitude variations with radiation for a finite time interval Δt are written explicitly in Eq. (64). On the limit of infinitesimal interval ($\Delta t\to dt$), Eq. (64) becomes, with the usual notation [11],

$$\frac{d|A_k|^2}{dt}=-2\alpha_k|A_k^2|+Q_k\ , \tag{65}$$

where α_k are the damping coefficients

$$\alpha_k = \left\langle \frac{P_\gamma}{2E_0} \right\rangle J_k \ , \tag{66}$$

which are proportional to the damping partition numbers J_k,

$$J_k = 1 + \left\langle \frac{\mathrm{Im}[(C_x \bar{w}_{1k} + C_z \bar{w}_{3k})(D_x w_{2k} - \dot{D}_x w_{1k} + D_z w_{4k} - \dot{D}_z w_{3k})]}{\mathrm{Im}(w_{1k}\bar{w}_{2k} + w_{3k}\bar{w}_{4k})} \right\rangle \ , \tag{67}$$

and where Q_k are the transverse beam amplitude coefficients

$$Q_k = \left\langle \frac{1}{4}\frac{Q_\varepsilon}{E_0^2} \right\rangle \left\langle \frac{|D_x w_{2k} - \dot{D}_x w_{1k} + D_z w_{4k} - \dot{D}_z w_{3k}|^2}{\mathrm{Im}^2(w_{1k}\bar{w}_{2k} + w_{3k}\bar{w}_{4k})} \right\rangle . \tag{68}$$

These relations use the identity $F(w_{jk}, \bar{w}_{jk}) = 2i\ \mathrm{Im}(w_{1k}\bar{w}_{2k} + w_{3k}\bar{w}_{4k})$.

Within the assumption made in Sec. IV A, a stationary state will occur after a few damping times and it corresponds to the condition $d|A_k|^2/dt = 0$. Hence the equilibrium amplitudes are [Eq. (65)]

$$|A_k^2| = \frac{Q_k}{2\alpha_k} \ , \tag{69}$$

and this is the important result to be used in Eq. (43). Betatron coupling is present through the eigenfunctions [Eq. (44)], the fact that both vertical and horizontal dispersions have an influence, and the need of four coefficients ($k = 1-4$) in order to describe the whole motion.

D. Equilibrium emittances with coupling and radiation

Betatron oscillations are characterized by the transverse invariants of the motion, which define the commonly used emittances E_y. If by definition E_y represents the invariant mean-square amplitudes of the transverse oscillations, we must have

$$E_y = \frac{\langle y^2 \rangle}{\beta_y} \ . \tag{70a}$$

Starting from the solution (43) and using the eigenfunctions (44) as well as the equalities between complex conjugates, we can rewrite Eq. (70a) in the following manner:

$$E_y = \frac{\langle y^2 \rangle}{\beta_y} = \frac{2}{\beta_y}(|A_1^2|\underset{31}{|w_{11}|^2} + |A_3^2|\underset{33}{|w_{13}|^2}) \ , \tag{70b}$$

the two subscripts of the w's being associated with the horizontal and the vertical coordinates, respectively.

In order to simplify the following calculations, let us now *assume* that the accelerator or the storage ring of interest is large and has separated functions. This means that the radius of curvature ρ is large and there is no gradient in the dipoles ($C_x \cong C_z \cong 0$). Consequently, $\langle D/\rho \rangle$ is small with respect to 1 and Eq. (66) becomes simply

$$\alpha_k = \left\langle \frac{P_\gamma}{2E_0} \right\rangle \tag{71}$$

with $J_k = 1$. Hence, putting together Eqs. (68)–(71) and introducing the explicit forms (44) of the eigenfunctions make it possible to write the emittances as

$$\begin{aligned} E_x &= \left\langle \frac{Q_\varepsilon}{RE_0P_\gamma} \right\rangle \left[\frac{4\omega_2^2|C^-|^2}{(4\omega_2^2 + |C^-|^2)^2}\langle H_1 \rangle + \frac{4\omega_1^2|C^-|^2}{(4\omega_1^2 + |C^-|^2)^2}\langle H_3 \rangle \right] , \\ E_z &= \left\langle \frac{Q_\varepsilon}{RE_0P_\gamma} \right\rangle \left[\frac{16\omega_2^4}{(4\omega_2^2 + |C^-|^2)^2}\langle H_1 \rangle + \frac{16\omega_1^4}{(4\omega_1^2 + |C^-|^2)^2}\langle H_3 \rangle \right] , \end{aligned} \tag{72}$$

where P_γ and Q_ε are given by Eqs. (55) and (60), respectively. It remains to define the functions H_1 and H_3, which are simply the numerator of the second bracket in Eq. (68) of Q_1 and Q_3:

$$\begin{aligned} \underset{3}{H_1} = {} & \frac{|C^-|^2}{\underset{1}{\omega_2^2}}\frac{R}{8\beta_x}\left[D_x^2 + \frac{1}{R^2}(\beta_x\dot{D}_x + R\alpha_x D_x)^2\right] + \frac{R}{2\beta_z}\left[D_z^2 + \frac{1}{R^2}(\beta_z\dot{D}_z + R\alpha_z D_z)^2\right] \\ & + \frac{R}{2\underset{1}{\omega_2}\sqrt{\beta_x\beta_z}}\mathrm{Re}[\bar{C}^-(\alpha_x - i)(\alpha_z + i)\exp(i\phi)]D_xD_z + \frac{\sqrt{\beta_x\beta_z}}{2\underset{1}{\omega_2}R}\mathrm{Re}[\bar{C}^-\exp(i\phi)]\dot{D}_x\dot{D}_z \\ & + \frac{1}{2\underset{1}{\omega_2}}\left[\frac{\beta_z}{\beta_x}\right]^{1/2}\mathrm{Re}[\bar{C}^-(\alpha_x - i)\exp(i\phi)]D_x\dot{D}_z + \frac{1}{2\underset{1}{\omega_2}}\left[\frac{\beta_x}{\beta_z}\right]^{1/2}\mathrm{Re}[\bar{C}^-(\alpha_z - i)\exp(i\phi)]\dot{D}_xD_z \ . \end{aligned} \tag{73}$$

The subscripts of H are associated with the two indices of ω [see Eq. (31)] and the phase ϕ is written for

$$\phi=\mu_x-\mu_z-\theta\Delta \ . \tag{74}$$

The two first terms of (73) are directly proportional to the dispersion invariants (named I_x and I_z), which appear naturally in E_x and E_z, respectively [11], in the absence of coupling. The other terms are obviously coupled terms for the dispersion.

Turning back to the expressions of the equilibrium emittances (72) and (73), which appear to be fairly complicated, let us look at two borderline cases.

(a) For vanishing linear coupling ($C^-\to 0$), the four terms in the square brackets of Eq. (72) have finite limits. Two of them are equal to zero, while the two remaining ones become equivalent to

$$\begin{aligned}\frac{4\omega_2^2|C^-|^2}{(4\omega_2^2+|C^-|^2)^2}\langle H_1\rangle&=\frac{R}{2}\langle I_x\rangle \ ,\\ \frac{16\omega_1^4}{(4\omega_1^2+|C^-|^2)^2}\langle H_3\rangle&=\frac{R}{2}\langle I_z\rangle \ .\end{aligned} \tag{75}$$

In this case, the transverse equilibrium emittances and their ratio $g=E_z/E_x$ are simply given by

$$E_y=\left\langle\frac{Q_\varepsilon}{2E_0P_\gamma}\right\rangle\langle I_y\rangle, \quad g=\frac{\langle I_z\rangle}{\langle I_x\rangle} \ . \tag{76}$$

As expected, the vertical emittance is nul, if the vertical dispersion vanishes in addition to C^-.

(b) For vanishing vertical dispersion (but $C^-\neq 0$), the functions (73) can be written as

$$H_{1,3}=\frac{|C^-|^2}{\omega_{2,1}^2}\frac{R}{8}\langle I_x\rangle \ . \tag{77}$$

Introducing Eq. (77) into Eq. (72) gives, for the emittances and their ratio g,

$$\begin{aligned}E_x&=\left\langle\frac{Q_\varepsilon I_x}{2E_0P_\gamma}\right\rangle\frac{\frac{1}{2}(|C^-|/\Delta)^2}{(|C^-|/\Delta)^2+1} \ ,\\ E_z&=\left\langle\frac{Q_\varepsilon I_x}{2E_0P_\gamma}\right\rangle\frac{\frac{1}{2}(|C^-|/\Delta)^2}{(|C^-|/\Delta)^2+1} \ ,\\ g&=\frac{(|C^-|/\Delta)^2}{(|C^-|/\Delta)^2+2} \ .\end{aligned} \tag{78}$$

The corresponding curves for E_x and g are plotted as functions of the ratio $|C^-|/2\Delta$ in Fig. 4. Both Eq. (78) and Fig. 4 show that in the limit $|C^-|\gg\Delta$ (sometimes called full coupling) the transverse emittances are equal and take half the value of the horizontal emittance at $C^-=0$. In general, coupling and vertical dispersion are not vanishing, so that not only I_x and I_z are contributing, but also the products D_xD_z, $\dot{D}_x\dot{D}_z$, $D_x\dot{D}_z$, and $\dot{D}_xD_z$, in agreement with expression (73).

V. APPLICATION TO LEP BETATRON COUPLING

In a circular collider like the LEP [12] with experiments installed around each interaction point, it is important to compensate for the linear coupling due to experimental solenoids [13] on the one side and the unavoidable sources of residual imperfections all around the ring on the other side. Coupling would indeed not only generate beating of the β function and tilting of the beam at crossing points, but also modify the nominal equilibrium emittances according to the mechanism described above, which in turn would influence the performance. Moreover, performance optimization requires an adjustment of the emittance ratio $g=E_z/E_x$, which can be achieved through variations of the coupling coefficient C^- (Sec. IV D) using a few specific tilted quadrupoles.

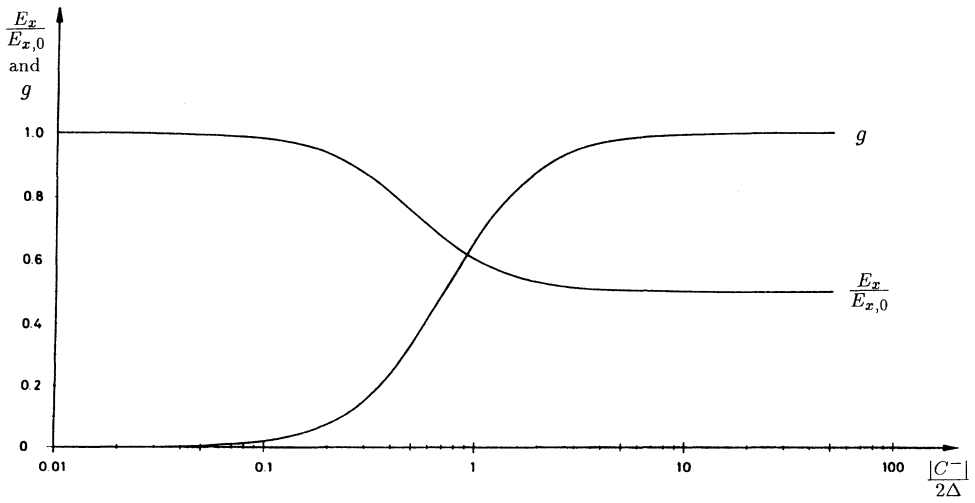

FIG. 4. Horizontal emittance and emittance ratio as function of $|C^-|/2\Delta$, with vanishing vertical dispersion. All quantities are dimensionless.

A. Emittance control with linear coupling

The performance of the LEP at a given beam current (limited by other mechanisms) is optimum when the beam-beam forces are such that the horizontal and the vertical beam-beam tune shifts are equal (and below a threshold of the order of 0.03 at collision). This implies the following relations between the emittances, the β^* functions, and beam sizes σ^* at the crossing point:

$$\frac{E_x}{E_z}=\frac{\beta_x^*}{\beta_z^*}=\frac{\sigma_x^*}{\sigma_z^*} . \tag{79}$$

The β^* ratio associated with the design of the experimental insertions (nominal value of 25 in the LEP) implies the use of flat beams and small values of g (4%). The expressions for the emittances in the presence of betatron coupling and radiation (Sec. IV D) allow an estimation of the range in which g can be controlled. The assumptions made in Sec. IV are fully valid for the LEP, which has tune values near a difference resonance (initial nominal tunes where $Q_x=70.4$ and $Q_z=78.3$, with a difference of 8 in the integers selected for beam-beam effect optimization), a very large radius of curvature, and a lattice with separated functions (i.e., $C_x=C_z=0$). If the horizontal dispersion invariant $\langle I_x \rangle$ has been estimated [13] to be equal to $1.75\ 10^{-2}$ m, the vertical one $\langle I_z \rangle$ is of the order of 1.8×10^{-4} m for a residual dispersion of approximately 10 cm (as expected in the best conditions), 11.2×10^{-4} m for D_z of 25 cm, and 28.8×10^{-4} m for D_z of 40 cm.

In these conditions, the theory developed above allows one to estimate the minimum emittance ratio [13], which can be reached for different amplitudes of the vertical dispersion. The best one can do consists of compensating exactly the linear coupling such as $C^-=0$. Equations (76) then apply directly and give minimum emittance ratios $g_{\min}$ of 1%, 6.25%, and 16%, for vertical dispersions of 10, 25, and 40 cm, respectively. The nominal conditions ($g=4\%$) imply that D_z must remain below approximately 20 cm. To get $C^-\cong0$ in LEP, there exist four tilted-quadrupole schemes located in sections where $D_x=0$, designed for the compensation of the fields of the experimental solenoids present at the collision points and for the control of the residual machine coupling [14].

In the other extreme case, the coupling coefficient can be so large that the contribution of the vertical dispersion to the emittance becomes negligible and Eqs. (78) apply. Using these equations and/or the curves of Fig. 4, one finds out that, for a distance to the difference resonance $\Delta=Q_x-Q_z+8$ of 0.1, values of 0.1, 0.2, 0.3, and 0.5 for C^- correspond to emittance ratios g of 33%, 66%, 82%, and 92% (all well above $g_{\min}$ associated with D_z only). The capacity of the LEP tilted-quadrupole schemes makes it possible to provide such high values of C^-, allowing either for full coupling if necessary and for compensation of contingently large C^- if required.

Looking at the numbers, the flat-beam configuration required for the LEP performance implies reducing the value of C^- below approximately 0.01 while keeping the residual amplitude of the vertical dispersion lower than ~10 cm. If the nominal value of $g=4\%$ is exceeded at constant beam current and insertion optics, the loss of luminosity will rise with approximately $\sqrt{g}$. Independently, a high value of C^- (>0.1 say) prevents accurately running of the ring and its injection system, since the optics is perturbed (in particular, for tunes close to a difference resonance) and the diagnostics are confused.

Among the possible sources of coupling to be compensated, most evident was an abnormally large betatron coupling discovered during early LEP commissioning. It manifested itself by coupling the first-turn trajectories, tilting and blowing up the beam and confusing tune measurements. All the necessary corrections were based on the formalism described above and can be used to illustrate its application.

B. Compensation of the ring linear coupling

Among the expected sources of linear coupling in the LEP, there are three that have been considered as important and estimated in the design phase. Indeed, the random tilts of all quadrupoles of rms value $\langle\theta\rangle$ and finite amplitudes of the vertical orbit (rms $\langle z\rangle$) in the systematic sextupoles required for chromaticity correction generate coupling, estimated to be

$$\begin{aligned} &|C^-|\cong0.009 \quad \text{for } \langle\theta\rangle=0.24 \text{ mrad} , \\ &|C^-|\cong0.012 \quad \text{for } \langle z\rangle=1.0 \text{ mm} \end{aligned} \tag{80}$$

on the nominal optics (tunes separated by 8). The third source was of course the experimental solenoids, of which the strongest field integral corresponds to $|C^-|\cong0.06$. This result justified the introduction of tilted quadrupoles near each interaction point (total of 8 per point) to reduce every solenoid contribution to below ~0.003.

There remain, however, sources due to field imperfections, initially considered as negligible, such as the field asymmetries in the magnets, the earth field, the induced current in a dissymmetric vacuum chamber, and the presence of magnetic material perturbing the field lines. One of those had to be responsible for the observed $|C^-|$ that was an order of magnitude higher than expected ($|C^-|\approx0.3$) and corresponded to a systematic skewed gradient of ~2 G m^{-1} in all arcs. Measurements ruled out the earth field as being the main contributor since the consequent skewed gradient estimated by including the shielding effect of the dipole is only about 0.15 G m^{-1}. The importance of asymmetries has not been precisely quantified, but the presence of ferromagnetic nickel in the contact layer between the aluminum chamber and the lead shield was identified as the main source of the unexpected perturbations [15]. The remanent field of the nickel can be strong and its component in the horizontal faces of the chamber creates an undesirable skewed field (Fig. 5).

In view of coupling compensation [16], it was first appropriate to reoptimize the linear optics of the LEP in order to modify the tune-integer separation (nominally equal to 8), for the collider was difficult to control and the source of imperfections had the periodicity 8 of the arcs. With tune integers separated by 6 ($Q_x=71.4$, $Q_z=77.3$),

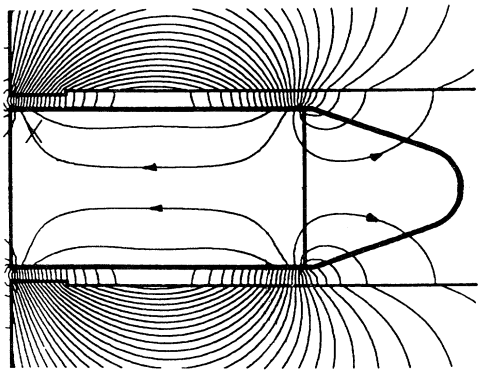

FIG. 5. Calculated field map in the LEP dipoles, due to nickel remanent field. The vacuum chamber is shown between the magnet poles (transversal section) and the nickel layer is on the surface of the chamber. The scale is given by the gap height separating the poles which is equal to 100 mm.

the driving term (15) of the difference resonance was reduced by approximately 5, but was still large

$$|C^-|=0.058 \quad \text{for } |Q_x-Q_z|=6\ . \tag{81}$$

The next step consisted of trying to compensate linear coupling by using the tilted quadrupoles already installed near each of the four experimental areas. For the necessary solenoid compensation, there are four pairs (or families) around every even crossing point able to entirely decouple betatron motions outside the experimental sections and at the interaction position. The corresponding pairs of magnets are termed QT1–QT4, the elements of a pair being symmetrically located with respect to the solenoid center. Antisymmetrically powered, these elements generate an imaginary component C^-, while they create a real component when powered with the same sign. The two pairs QT2 and QT3 are antisymmetrically powered to mainly compensate for the solenoids (imaginary C^-; see Sec. V C), while the magnets of QT1 and QT4 are independent in order to give means of compensating ring imperfections (mainly real C^-). The margin in their strengths, foreseen for running at $\sim$100 GeV, made it possible to use them for correcting the strong systematic coupling due to the vacuum chamber at injection.

Since the working point of the LEP is close to a difference resonance, the efforts for correcting the ring imperfections were focused on a reduction of C^-. Measurements basically concerned with the normal mode frequencies (Sec. III B) and predictions of corrections were based on estimates of C^- using Eqs. (15) and (16), as well as on numerical simulations.

The first successful compensation was obtained using the optics with $|Q_x-Q_z|=6$ and the QT1 tilted quadrupoles [17]. It was based on the observation supported by numerical simulations that a second harmonic of a skewed-gradient correction had strong effects on coupling with this optics, for the source of the imperfections was mainly harmonic 8. Subsidiarily, two arcs enclosing one crossing point and having approximately symmetrical errors generate a real component C^- at this point, as can be seen from formula (15) using the appropriate phases. Both arguments incited us to excite the QT1 according to the following pattern (e.g., L2 stands for left of point 2 and R2 for right of point 2),

Position	L2	R2	L4	R4	L6	R6	L8	R8
QT1 polarity	−	−	+	+	−	−	+	+

QT1 absolute normalized strength 0.006 m^{-2} at 20 GeV.

This first "historical" compensation [16,17] succeeded in decreasing $|C^-|$ by more than an order of magnitude, down to 0.001, as shown in Fig. 6 (with experimental solenoids switched off). The corresponding change in the beam aspect ratio, at positions with and without horizontal dispersion (top and bottom), can be seen in Fig. 7. This correction made the control of the machine much easier and physics runs successful. Later, compensation was achieved by using the QT4 quadrupoles, which are almost equivalent but the tuning of which do not depend on the betatron amplitudes at the interaction points. The compensation was also distributed in the arcs by adding pairs of small tilted quadrupoles near the center of each arc. All these schemes were based on the treatment recalled in Sec. II [2].

Given the limited resolution of the information conveyed by the luminescent screens (Fig. 7), the careful comparison of the two pictures at $D_x=0$ and at finite D_x (assumed to be close to the nominal value) allowed a rough estimate of the actual emittance ratio. Hence what seems to be full coupling on the bottom left picture before compensation corresponds to an emittance ratio g of $\sim$0.3. Similarly, the bottom right picture taken after compensation conceals a ratio about two times smaller (in agreement with the observed vertical dispersion of about 40 cm, as pointed out in Sec. V A). The ring compensation done as explained made possible further optical adjustments and correction of solenoid effects (Sec. V C), leading to a rise of luminosity (an order of magnitude, say). After reducing D_z by careful orbit corrections to about 20–25 cm, the emittance ratio approached the nominal 4% (Sec. V A) and the expected luminosity was within reach. Even though the betatron coupling due to the magnetization of the nickel layer of the LEP dipole

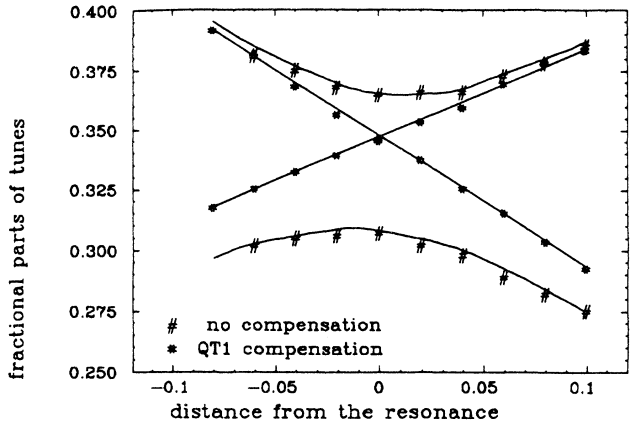

FIG. 6. Tune separation on the difference resonance, before and after the first compensation with the tilted quadrupoles QT1 of LEP (dimensionless quantities).

vacuum chamber has been much weakened as described, the source itself has been suppressed more recently [15] by demagnetizing the nickel layer of the chamber, reducing the bare coupling by more than a factor 5.

C. Compensation of solenoid linear coupling

Let us here differentiate between the coefficients arising from tilted quadrupoles and from solenoids by $C_{SQ}^{\pm}$ and $C_{\rm sol}^{\pm}$. Now the requirement of full compensation of solenoidal effects with tilted quadrupoles may be formulated easily

$$C_{\rm sol}^{\pm}+\sum C_{SQ}^{\pm}=0\ . \tag{82}$$

The summation has to be made over all tilted quadrupoles that are excited to compensate the solenoids.

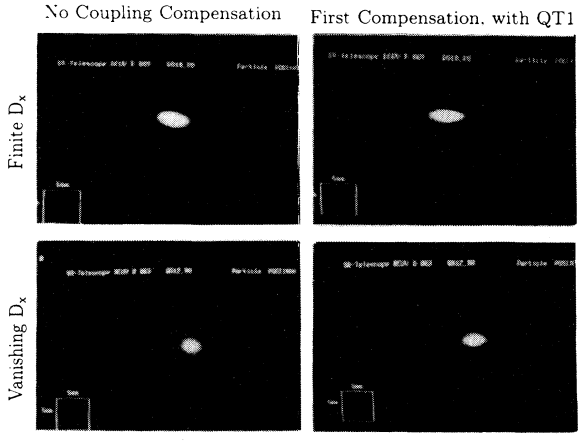

FIG. 7. Beam aspect from the light monitors placed at finite or vanishing dispersion, before and after the first coupling compensation in LEP (transversal beam section). The squares on the pictures have 5-mm sides.

Hence there are four linear equations since C^+ and C^- are complex and, in a thin-lens approximation for the tilted quadrupoles only, the system (82) may be written as follows [14,18] by virtue of (16) and Eq. (15c) (with $S=0$):

$$\sum_j \frac{1}{2\pi R^2}[\sqrt{\beta_x\beta_z}Kl]_j \times\cos\left[\mu_x-\mu_z-\frac{s}{R}\Delta^{\mp}\right]_j+C_{\rm sol,1}^{\mp}=0\ , \tag{83}$$

$$\sum_j \frac{1}{2\pi R^2}[\sqrt{\beta_x\beta_z}Kl]_j \times\sin\left[\mu_x-\mu_z-\frac{s}{R}\Delta^{\mp}\right]_j+C_{\rm sol,2}^{\mp}=0\ ,$$

where s is the quadrupole position and l the quadrupole length. K is defined by (1). Equations (83) correspond to the real and the imaginary components of $C^{\mp}$ (indices 1 and 2, respectively) and are valid for either the difference or the sum resonance. In the case of a solenoid with a pure longitudinal field and centered at the minimum of the betatron functions, the coupling coefficients can be derived analytically from Eqs. (15) (with $K=0$ and $S\neq 0$). The variations of the "Twiss functions" α_y, β_y, and μ_y in a drift space are known to be

$$\beta_y(s)=\beta_y^*+\frac{s^2}{\beta_y^*},\quad \alpha_y=-\frac{s}{\beta_y^*},\quad \mu_y=\arctan\frac{s}{\beta_y^*}\ , \tag{84}$$

where the asterisk denotes the parameter values at the minimum of the betatron amplitude, chosen as the origin of s. Inserting these expressions in the integral (15) gives the simple solution [18]

$$C_{\rm sol}^{*\mp}=-i\frac{SL}{\pi R}\left[\left[\frac{\beta_z^*}{\beta_x^*}\right]^{1/2}\mp\left[\frac{\beta_x^*}{\beta_z^*}\right]^{1/2}\right], \tag{85}$$

where L is the length of the solenoid and S is defined by (2). Both vectors are purely imaginary in the chosen coordinate system. Their cancellation then imposes the use of pairs of skewed quadrupoles symmetrically placed with respect to the interaction point and having opposite currents, because C_{SQ} (left) is the complex conjugate of C_{SQ} (right). The presence of a real component due to ring imperfections or overlap of one solenoidal field with the next focusing quadrupoles (for example, the L3 experiment in the LEP) requires, however, the presence of two pairs of symmetrical quadrupoles with independent power supplies to allow currents of the same or opposite sign. All these considerations, the four conditions (83) linked to the expressions (85) and the particular values of the phases μ_y and functions β_y, induced us to choose the scheme shown in Fig. 8 for half an insertion [18]. It can be used to compensate either the solenoids or the ring, as explained in Sec. V A.

Let us underline here that this scheme makes it possible to decouple the motions at the solenoid centers, in order to avoid any distortion of the four-dimensional beam ellipsoid, which could reduce performance and luminosity. Moreover, the simultaneous compensation of C^+ and C^- outside the insertion of Fig. 8 and at the interaction

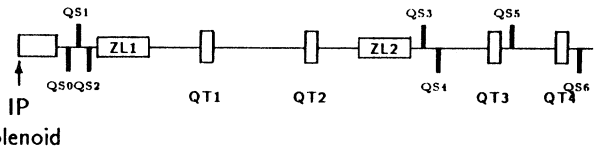

FIG. 8. Half LEP insertion with the experimental solenoid, the tilted quadrupoles (QT) for compensation, the focusing quadrupoles (QS), and the vertical electrostatic separators (ZL).

point prevents the existence of tilted normal modes and β_y beating in these positions and in the arcs [18]. Neglecting C^+ would indeed let a perturbation develop according to Eqs. (28), and it can be interpreted as a modulation of the β_y function, considering the form of the complete solution that is similar to (31). This modulation is the more important the stronger is the tilt of the normal modes, i.e., the modifications (29) or (30) of the wave numbers. The effect is therefore a function of the ratio $|C^+|/\Delta^+$ and decreases with increasing Δ^+. It is, however, never completely negligible even when the working point is roughly centered between two sum resonance lines.

Only the compensation of both C^+ and C^- avoid this imperfection and completely decoupled the transfer matrix across an experimental insertion. This fact was numerically tested [18] for one particular LEP solenoid, using the programs TRANSPORT and PETROS. TRANSPORT simulates the propagation of the beam ellipsoid throughout an insertion and PETROS simulates the beam dynamics of the whole machine with a compensated solenoid. TRANSPORT confirmed that the beam sizes at the crossing were not perturbed by more than 0.5% after compensation and PETROS showed that the tilt of normal modes was below 0.005° at the crossing and 0.04° in the arcs.

The four solenoids to be compensated in the LEP are

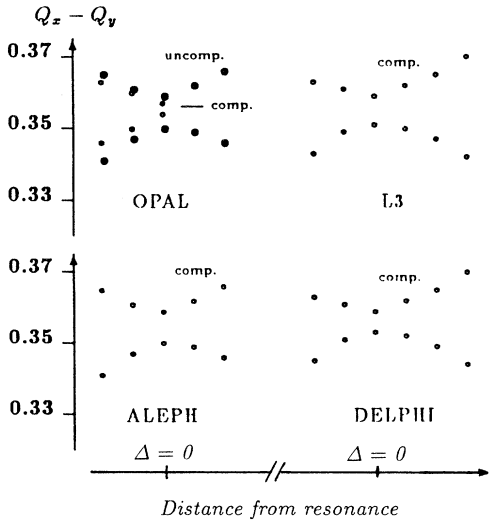

FIG. 9. Residual tune separations measured after initial compensation of each experimental magnet in LEP. Quantities are dimensionless.

those of the experiments L3, ALEPH, OPAL, and DELPHI, with difference coupling ranging from 0.015 to 0.06. Compensation with the scheme described was precalculated according to the present theory and initially set up. These corrections were successful in general, but some experimental adjustments were required sometimes to get a residual $|C|$ between 0.003 and 0.006 [14]. These might, however, correspond to a general minimization of the actual coupling around the ring rather than to a local correction. The outcome was checked by measuring $|C^-|$ with the method of Sec. III B and individual results obtained in the early commissioning phase are displayed in Fig. 9.

[1] G. Guignard, in *Physics of Particle Accelerators,* edited by Melvin Month and Margaret Dienes, AIP Conf. Proc. No. 184 (AIP, New York, 1989), Vol. 1, pp. 822–890.
[2] G. Guignard, CERN Report No. 76-06, 1976 (unpublished).
[3] G. Ripken, DESY Report No. R1-70/4, 1970 (unpublished).
[4] A. Schoch, CERN Report No. 57-21, 1957 (unpublished).
[5] R. Hagedorn, CERN Report No. 57-1, 1957 (unpublished).
[6] P. J. Bryant, CERN Report No. ISR-MA/75-28, 1975 (unpublished).
[7] G. Guignard, CERN Report No. ISR-BOM/77-43, 1977 (unpublished).
[8] K. Takikawa, CERN Report No. ISR-MA/75-34, 1975 (unpublished).
[9] P. J. Bryant and G. Guignard, CERN Report No. ISR-MA/75-42, 1975 (unpublished).
[10] A. Piwinsky (private communication).
[11] M. Sands, Stanford Linear Accelerator Center Report No. SLAC-121, 1970 (unpublished).
[12] LEP Report No. CERN-LEP/84-01, 1984 (unpublished).
[13] G. Guignard, in *Proceedings of the 11th International Conference on High-Energy Accelerators, CERN, Geneva, 1980,* edited by W. S. Newman (Birkhäuser, Basel, 1980), p. 682.
[14] G. Guignard *et al.*, in *Proceeding of 2nd European Particle Accelerator Conference, Nice, 1990,* edited by P. Marin and P. Mandrillon (Editions Frontières, Gif-sur-Yvette, France, 1990), Vol. 2, p. 1432.
[15] J. Billan *et al.*, in *Proceedings of the 1993 Particle Accelerator Conference, Washington, DC,* edited by Steven T. Corneliussen (The Institute of Electrical and Electronics Engineers, Piscataway, NJ, 1993), Vol. 1, p. 68.
[16] J. P. Gourber, G. Guignard, A. Hofmann, J. P. Koutchouk, and H. Moshammer, *Proceeding of 2nd European Particle Accelerator Conference, Nice, 1990,* edited by P. Marin and P. Mandrillon (Editions Frontières, Gif-sur-Yvette, France, 1990), Vol. 2, p. 1429.
[17] G. Guignard, in *Particles and Fields Series 48,* edited by Alex Chao, AIP Conf. Proc. No. 255 (AIP, New York, 1992), Vol. 2, p. 3.
[18] G. Guignard (private communication).

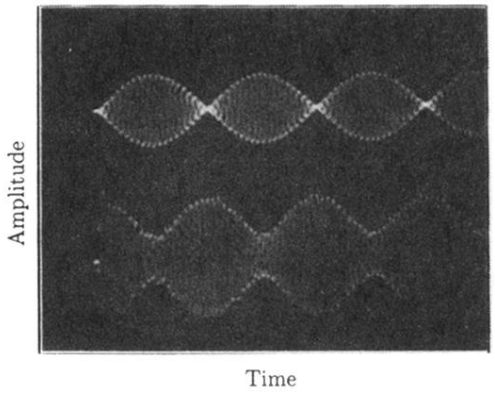

FIG. 2. Vertical (above) and horizontal (below) coherent oscillations measured in the Intersecting Storage Rings (CERN) after a horizontal kick. The beating period is 0.5 ms in this case.

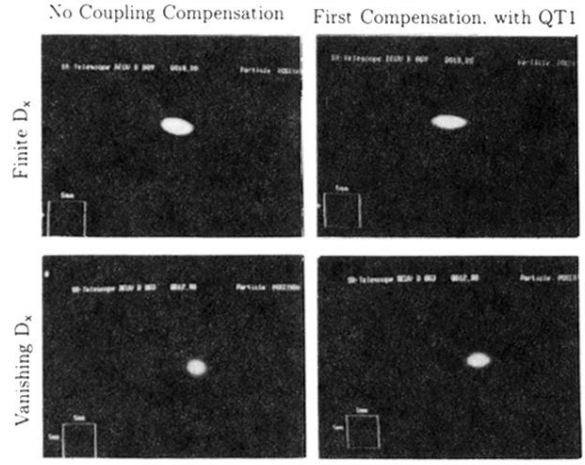

FIG. 7. Beam aspect from the light monitors placed at finite or vanishing dispersion, before and after the first coupling compensation in LEP (transversal beam section). The squares on the pictures have 5-mm sides.